# Design of a Novel Compact Dual-band Wilkinson Power Divider with Improved Isolation

Hao Zhang, Wei Kang, and Wen Wu, *Senior Member, IEEE*
the Ministerial Key Laboratory, JGMT, Nanjing University of Science and Technology
Nanjing 210094, China

***Abstract*-A dual-band Wilkinson power divider with a novel compact structure has been presented. This new structure consists of three transmission lines, a short stub and RCL components. Due to the existence of the RCL circuit, better output match and isolation are obtained. Even- and odd-mode analysis and ABCD-matrix are used to get the design equations. The miniaturized power divider which working at 1 and 2.5 GHz has an area of only 3.2 × 2.4 cm$^2$. Its experimental results show an excellent agreement with theoretical results.**

## I. Introduction

The Wilkinson divider is an important component in radio front-ends, which is a hot research topic in the RF field. Recently, various dual-band Wilkinson power dividers are put forward to meet the demand of the dual-band operations.

A dual-band power divider using two section lines has been developed in [1] with poor output return loss and isolation. In [2]-[5], a series or parallel RCL circuit is introduced on the basic of [1]. Fig. 1 shows the traditional unequal dual-band power divider with a series RCL circuit in [4]. Using this structure, equal power divider can not be designed unless with coupled lines. Both open- and short-ended stubs are applied in [6] to obtain flexible frequency ratios. In [7], two coupled lines and two lumped resistors have been used in the dual-band operations. Non-uniform transmission lines used in a compact dual-band power divider has been presented in [8].

In this letter, a new dual-band Wilkinson power divider is presented. The important features include: 1) Miniaturization design. 2) Flexible layout design. 3) Excellent amplitude balance. These three characteristics are described in detail in the following. In section II, the design principle and the method are introduced to clarify the design philosophy. An example, simulated results, measured results and conclusions follow in sections III and IV.

## II. Theory Analysis and Design Equations

Fig. 1 shows the conventional dual-band Wilkinson power divider with a series RCL circuit in [4], it has a perfect input return loss but a poor output return loss mainly due to the difficult welding of three series lumped elements. An extra impedance matching circuit of each port also makes it a larger size. This structure can not be used to design the equal power divider unless with coupled lines. Then, we present a new compact one in Fig. 2 which shows the assumption diagram of the dual-band equal power divider. We add a short stub in parallel with port 1 and change the way in series and parallel of the RCL circuit. Also, we put two pads in the welding points between the capacitance and the inductance respectively to reduce the difficulty of welding. Unlike many other typical dual-band power dividers, it's very compact due to only three transmission lines and a short stub. The resistor is used to obtain output match and good isolation, and the series LC circuit is used to achieve output match at two different frequencies. Even- and odd-mode analysis is applied to acquire design equations of the power divider.

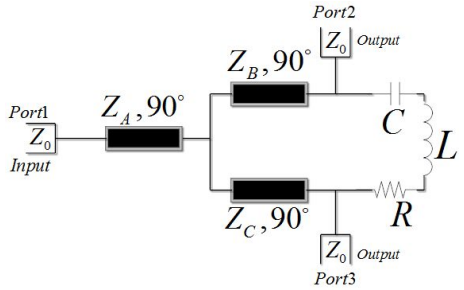


Fig 1. Conventional dual-band Wilkinson power divider.

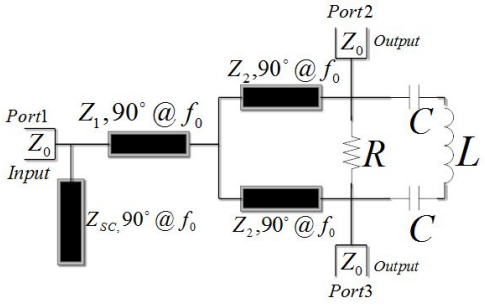


Fig 2. Proposed dual-band Wilkinson power divider.

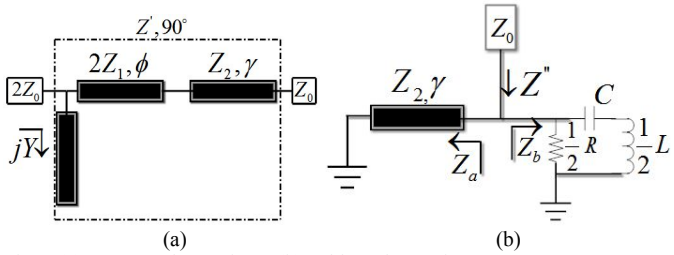


Fig 3. (a) Even-mode topology. (b) Odd-mode topology.

### *A. Even-Mode Analysis*

978-1-4673-8983-9/16/$31.00 ©2016 IEEE

According to the symmetrical structure in Fig. 2, there is no current flowing through the plane of symmetry. Fig. 3(a) paints the even-mode structure which is made up with a two-section branch-line and a stub line (*Y*). Also, no current flows through the lumped elements between the two output ports which can be omitted. The impedance at port 1 is doubled according to the even-mode analysis. In the mathematical calculation, it is convenient to solve the problem using ABCD-matrix. According to the microwave network theory, we can obtain from Fig. 3(a) that

$$\begin{bmatrix} 1 & 0 \\ jY & 1 \end{bmatrix} \begin{bmatrix} \cos\varphi & j2Z_1 \sin\varphi \\ \dfrac{j\sin\varphi}{2Z_1} & \cos\varphi \end{bmatrix} \begin{bmatrix} \cos\gamma & jZ_2 \sin\gamma \\ \dfrac{j\sin\gamma}{Z_2} & \cos\gamma \end{bmatrix} = \begin{bmatrix} 0 & jZ' \\ \dfrac{j}{Z'} & 0 \end{bmatrix} \tag{1}$$

Where *Y* is the admittance of the stub line.

After doing a few algebraic operators, the above matrix equation is divided into the following equations

$$Z' = \sqrt{2}Z_0 \tag{2}$$

$$Z_2 = Z' \frac{\sin\gamma}{\cos\varphi} \tag{3}$$

$$Z_1 = \frac{Z_2}{2\tan\varphi \cdot \tan\gamma} \tag{4}$$

$$Y = \frac{\cos(\varphi+\gamma)\cos(\varphi-\gamma)}{Z'\cos\varphi\cos\gamma}. \tag{5}$$

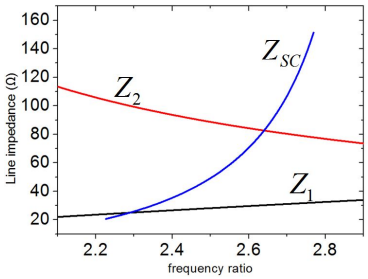


Fig 4. Line impedance versus frequency ratio.

*B. Odd-Mode Analysis*

Fig. 3(b) depicts the structure for odd-mode analysis. There is a virtual ground along the middle of the circuit. Following the transmission line theory, the characteristic impedance $Z_a$ and $Z_b$ in Fig. 3(b) are given by

$$Z_a = Z_2 \frac{0 + jZ_2 \tan\gamma}{Z_2 + j\cdot 0 \cdot \tan\gamma} = j \cdot Z_2 \tan\gamma \tag{6}$$

$$Z_b = \frac{\frac{1}{2}R \cdot (\frac{1}{j\omega c} + j\cdot\frac{1}{2}\omega L)}{\frac{1}{2}R + (\frac{1}{j\omega c} + j\cdot\frac{1}{2}\omega L)} = \frac{2R - \omega^2 LCR}{j\cdot 2\omega CR + 4 - 2\omega^2 LC}. \tag{7}$$

Finally, the equivalent resistance matches the impedance $Z_0$

$$Z'' = \frac{Z_a \cdot Z_b}{Z_a + Z_b} = Z_0. \tag{8}$$

The real and the imaginary parts are equal respectively, we can obtain

$$R = 2Z_0 \tag{9}$$

$$2Z_2\omega c \tan\gamma + \omega^2 LC = 2. \tag{10}$$

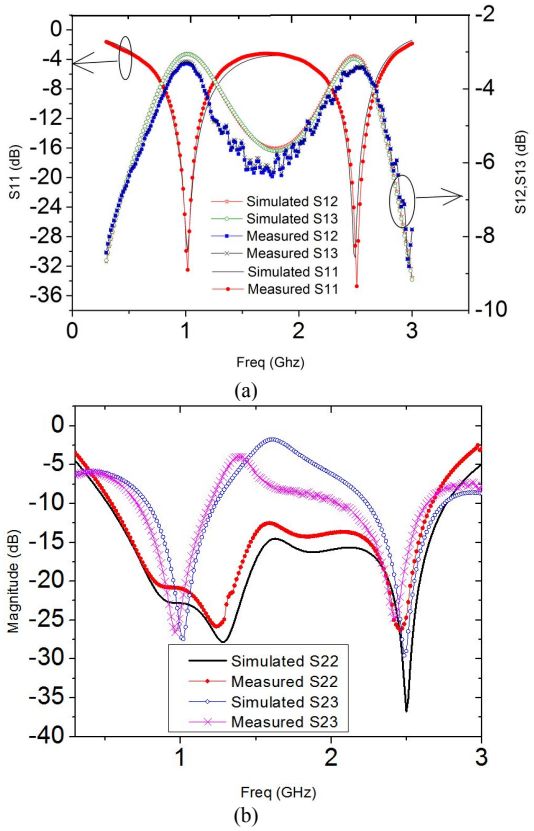


Fig 5. Simulated and measured results: (a) *S*11, *S*12 and *S*13, (b) *S*22 and *S*23.

C. *Dual-band Analysis*

Assuming the low working frequency of the dual-band power divider is $f_1$, the other is $f_2$ and $f_2 = m \cdot f_1$ ($m$ is the frequency ratio, m>1), from [1], we can get

$$\tan\gamma_{f_1} = -\tan\gamma_{f_2} \tag{11}$$

$$\gamma_{f_1} = \frac{\pi}{1+m}, \gamma_{f_2} = \pi - \gamma_{f_1} = \frac{m\pi}{1+m}. \tag{12}$$

Using algebraic processing method, we determine

$$\phi(f_1) = \gamma(f_1) = \frac{\pi}{2}\frac{f_1}{f_0} = \frac{\pi}{2}(1-\theta) \tag{13}$$

$$\phi(f_2) = \gamma(f_2) = \frac{\pi}{2}\frac{f_2}{f_0} = \frac{\pi}{2}(1+\theta) \tag{14}$$

$$\theta = \frac{f_2/f_1 - 1}{f_2/f_1 + 1} = \frac{m-1}{m+1}, f_0 = \frac{f_1 + f_2}{2}. \tag{15}$$

By substituting (13) and (14) into (3)-(5), we obtain

$$Z_1 = \frac{\sqrt{2}}{2} Z_0 \tan\frac{\pi}{2}\theta \tag{16}$$

$$Z_2 = \sqrt{2}Z_0 \cot\frac{\pi}{2}\theta \tag{17}$$

$$\frac{1}{jY} = j2Z_{SC}\tan\frac{\pi}{2}(1+\theta) \tag{18}$$

$$Z_{SC} = \frac{Z_0}{2}\frac{\tan\pi\theta}{\sqrt{2}}\tan^2\frac{\pi}{2}\theta. \tag{19}$$

Put $w_1$, $w_2$, $\tan\gamma_{f1}$, $\tan\gamma_{f2}$ into (10), we get

$$L = \frac{2Z_2 \tan\gamma}{2\pi(f_2 - f_1)}, \quad C = \frac{(f_1 - f_2)}{2\pi f_1 f_2 Z_2 \tan\gamma}. \tag{20}$$

TABLE I
PERFORMANCE INDICATORS VERSUS DIFFERENT CIRCUIT TOPOLOGIES

| | Working frequency | Port isolation (dB) $S23$ | Amplitude balance (dB) $S21$-$S31$ | Phase balance $\angle S21$-$\angle S31$ | Size ($\lambda_0^2$) |
|---|---|---|---|---|---|
| [2] | $f_1$=1Ghz<br>$f_2$=4Ghz | -18<br>-30 | 0.17<br>0.24 | - | 0.193 |
| [6] | $f_1$=1.8Ghz<br>$f_2$=5.8Ghz | -29<br>-17 | -0.23<br>-0.22 | 0.42°<br>-0.17° | - |
| [7] | $f_1$=1.1Ghz<br>$f_2$=2.2Ghz | -37<br>-36 | 0.04 | - | 0.053 |
| This work | $f_1$=1Ghz<br>$f_2$=2.5Ghz | -28<br>-27 | -0.06<br>-0.03 | 0.42°<br>0.61° | 0.026 |

Fig. 4 shows the relationship between line impedance ($Z_1$, $Z_2$, $Z_{SC}$) and frequency ratio ($m$). It suggests that the power divider can wok at a frequency ratio ranging from 2.2 to 2.75 with the right choice of proper topology.

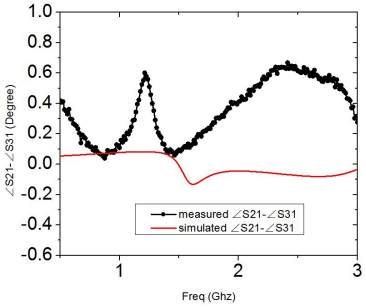


Fig 6. Simulated and measured phase responses.

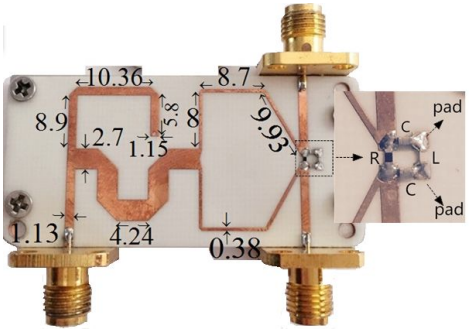


Fig 7. Fabricated Wilkinson power divider and dimensions of the transmission lines. (units: mm)

## III. SIMULATED AND EXPERIMENTAL RESULTS

In order to prove the above theory, we design a dual-band power divider operating at both 1 and 2.5 GHz on a substrate with a dielectric constant of 3.55. Through the calculation of the above equation, the design parameters for this novel dual-band Wilkinson power divider are given as $Z_1$=28.17 Ω, $Z_2$=88.72 Ω, $Z_{SC}$=49.04 Ω, $R$=100 Ω, $C$≈0.85 pF, and $L$≈23.6 nH.

Fig. 5 shows the comparisons between the simulated and measured results. The simulation and optimization are completed by the Ansoft HFSS 12.0 and the measurement is implemented using N5224A (PNA Network Analyzer) from Agilent Technologies. From the above data, we find that the simulations and the measurements have an excellent agreement. Fig. 6 presents the phase responses and the phase balance between ports 2 and 3 is shown in table I. Small discrepancies are existent mainly caused by the limited machining accuracy and the measurement error. Moreover, input return loss of over 32 dB is found at the two center frequencies and the insertion loss is less than 3.2 dB. Port isolation, amplitude balance, phase balance and the size are listed clearly in table I.

Compared with other designs, the new structure has more advantages on amplitude balance and miniaturization. Two pads are put in the welding points between the capacitance and the inductance respectively. Through appropriate adjustment with the size of welding plate, the measured results of the output return loss matches better with the simulated ones than those in [4]. Fig. 7 shows the photograph of the fabricated power divider which has an area of 3.2 × 2.4 cm$^2$. It's only possessing 35.3 % of the traditional two-section dual-band power divider in [2] whose area is 6.4 × 3.4 cm$^2$. Dimensions of the transmission lines are clearly presented in Fig. 7. The transmission line whose width is 2.7 mm has been divided into five microstrip lines of the same length.

## IV. CONCLUSION

A new structure for the dual-band power divider is discussed in this paper. This circuit can obtain great electrical performance. The introduction of RCL circuit not only has a great effect on the isolation between the two output ports, but more reaches the optimal output return loss. The capacitance caused by the two added pad, the fabrication process and the coupling factor of the microstrip line are the main point which leads to the small discrepancies between the measured and simulated results.

## REFERENCES


[1] C. Monzon, "A small dual-frequency transformer in two section," *IEEE Trans. Microw. Theory Tech.,* vol. 51, no. 4, pp. 1157–1161, Apr. 2003.

[2] L. Wu, Z. Sun, H. Yilmaz and M. Berroth, "A dual-frequency Wilkinson power divider," *IEEE Trans. Microw. Theory Tech.,* vol. 54, no. 1, pp. 278-284, Jan. 2006.

[3] Xiaolong Wang, Iwata Sakagami, Kensaku Takahashi and Shingo Okamura, "A Generalized Dual-Band Wilkinson Power Divider With Parallel L, C and R Components," *IEEE Trans. Microw. Theory Tech.,* vol. 60, no. 4, pp. 952-964, Apr, 2012.

[4] Xiaolong Wang and Iwata Sakagami, "Generalized Dual-Frequency Wilkinson Power Dividers with a Series/Parallel RCL Circuit," *Microw. Symposium Digest (MTT),* pp. 1-4, 2011.

[5] L. Wu, H. Yilmaz, T. Bitzer, and A. Pascht. M. Berroth, "A Dual-Frequency Wilkinson Power Divider: For a Frequency and Its First Harmonic," *IEEE Microw. Wireless Compon. Lett.,* vol. 15, no. 2, pp. 107-109, Feb, 2005.

[6] Hualiang Zhang and Hao Xin, "Designs of Dual-Band Wilkinson Power Dividers with Flexible Frequency Ratios," *Microw. Symposium Digest, 2008 IEEE MTT-S International,* pp. 1223 - 1226, June, 2008.

[7] Yongle Wu, Yuanan Liu and Quan Xue, "An Analytical Approach for a Novel Coupled-Line Dual-Band Wilkinson Power Divider," *IEEE Trans. Microw. Theory Tech.,* vol. 59, no. 2, pp. 286-294, Feb, 2011.

[8] Y.-F. Bai, X.-H. Wang, C.-J. Gao, X.-W. Shi and H.-J. Lin, "Compact dual-band power divider using non-uniform transmission line," *Electronics letters,* vol. 47, no. 3, pp. 188-190, 2011.